Article:

Hu, H. orcid.org/0000-0002-7767-0016, Zhang, B., Hong, Q. et al. (2 more authors) (2018) Coverage Analysis of Reduced Power Subframes Applied in Heterogeneous Networks with Subframe Misalignment Interference. IEEE Wireless Communications Letters, 7 (5). pp. 752-755. ISSN 2162-2337

https://doi.org/10.1109/LWC.2018.2818176

Coverage Analysis of Reduced Power Subframes Applied in Heterogeneous Networks with Subframe Misalignment Interference

Haonan Hu[1,2], Baoling Zhang[2], Qi Hong[2], Xiaoli Chu[2] and Jie Zhang[2]

***Abstract*—In heterogeneous networks (HetNets), to reduce the interference to users in Cell Range Expansion (CRE) areas of small cells, Reduced Power Subframes (RPSs) are used by macro base stations (BSs) to serve their center region users. CRE users can receive full power subframes (FPSs) from small-cell BSs in the same time slots as RPSs. However, it is difficult to maintain strict subframe alignment (SA) between neighbouring cells. Subframe misalignment (SM) between RPSs and FPSs transmitted by neighbouring macro BSs and small-cell BSs may degrade the coverage performance for macrocell center and small-cell CRE users. With existing time synchronization techniques used in HetNets, the SM offsets are actually upper-bounded. In this letter, we propose a novel SM model for a two-tier HetNet adopting RPSs with SM offsets restricted within a subframe duration, and analyse the coverage probability under the effects of RPSs and SM based on stochastic geometry. The results show that the strict SA requirement can be relaxed by up to 20% of subframe duration with below 5% coverage loss.**

***Index Terms*—subframe misalignment, reduced power subframes, stochastic geometry, heterogeneous networks**

I. Introduction

In heterogeneous networks (HetNets), due to the difference in downlink transmit power between different tiers, cell range expansion (CRE) has been proposed to extend the coverage areas of small cells by using a range expansion bias without increasing their transmit power. However, small-cell CRE users become vulnerable to interference from macrocells. Almost blank subframes (ABSs) [1], with no transmit power on data channel, were used in macrocells, so that small-cell CRE users can receive full power subframes (FPSs) in the same time slots as ABSs without suffering from significant interference from macro base stations (BSs). Nevertheless, this technique will cause significant capacity loss to macrocells. In order to reduce the capacity loss, reduced power subframes (RPSs) [2], with a relatively low transmit power as compared with FPSs, have been proposed to serve macrocell center region users, while mitigating the interference to small-cell CRE users. However, the use of RPSs requires strict subframe alignment (SA), which cannot always be satisfied. The SA between macrocells and small cells is achieved through control signal exchanges via the backhaul [3], which may be congested in a high density scenario. Moreover, due to random propagation delays, subframes transmitted from neighbouring cells may be misaligned, namely subframe misalignment (SM). Because of SM, macrocell center and small-cell CRE users may suffer increased interference from FPSs, which degrades their coverage performance.

In [2], it was shown that RPSs can increase the total network capacity of a two-tier HetNet, assuming no RPSs transmitted from neighboring cells. In [4], it was shown that with a static range expansion, RPSs outperform ABSs in terms of the average rate of a user under strict SA. In [5], the downlink coverage with asynchronous slots was studied in a two-tier HetNet, where the offsets of unsynchronized slots may take arbitrarily large values. However, by employing existing time synchronization techniques via the backhaul, the offsets of unsynchronized slots may not exceed a slot duration [6]. The offsets of unsynchronized slots can be considered as the SM offsets, since a subframe consists of two slots in an orthogonal frequency-division multiple access (OFDMA) network. Accordingly, the SM offsets are also restricted in a specific range, and the maximum value of this range is defined as the maximum subframe misalignment offset (MSMO).

In this letter, we analyse the effect of SM on the coverage probability in a two-tier HetNet adopting RPSs. We propose an SM model with the misalignment offsets restricted by the MSMO, which is a more practical misalignment model than that in [5]. Based on this proposed SM model, the downlink coverage probability for a typical user is derived based on stochastic geometry and validated through Monte Carlo simulation. By analysing the coverage degradation caused by SM versus the subframe duration, we provide design insights into the SA requirement for using RPSs in HetNets.

II. System Model

We consider a two-tier HetNet, where macro BSs form tier 1 and small-cell BSs form tier 2. Define $\mathcal{K} = \{1, 2\}$. For a BS in the i-th tier, $i \in \mathcal{K}$, the transmit power in an FPS is P_i, and the transmit power in an RPS is $\rho_i P_i$, where $\rho_i (0 < \rho_i \leq 1)$ is the power reduction factor. The proportion of RPSs among all transmitted subframes, which is defined as the duty cycle, is β_i and can be considered as the probability of a subframe being an RPS. We assume that small-cell BSs transmit at full power in RPSs, i.e., $\rho_2 = 1$. The positions of the i-th tier BSs are modelled as an independent spatial Poisson point process (PPP) Φ_i, with the density of λ_i, $i \in \mathcal{K}$. The locations of users

This work acknowledges the support of the MOST of China (Project No. 2015DFE12820), the is3DMIMO (Project No. 734798), and the China Scholarship Council.

[1]H. Hu is with the School of Communication and Information Engineering, Chongqing University of Posts and Telecommunications, Chongqing 400065, China (e-mail:haonan.hu@sheffield.ac.uk). [2]H. Hu, B. Zhang, Q. Hong, X. Chu and J. Zhang are with the Department of Electronic and Electrical Engineering, The University of Sheffield, Sheffield S10 2TN, UK.

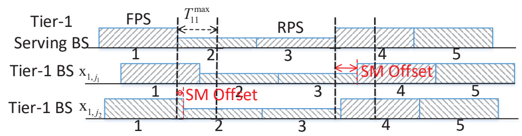

Fig. 1. SM between tier-1 serving BS and tier-1 interfering BSs

are modelled as another independent spatial PPP. According to Slivnyak's theorem [7], we assume a typical user located at the origin without loss of generality. The location of the j-th BS in the i-th tier is denoted by $\mathbf{x}_{i,j}$, and its distance to the typical user is given by $r_{i,j} = ||\mathbf{x}_{i,j}||$. The corresponding pathloss is given by $r_{i,j}^{-\alpha_i}$, where α_i is the i-th tier pathloss exponent. We assume independent Rayleigh fading for each link, thus the fading power gain $h_{i,j}$ on the link from the j-th BS in the i-th tier to the typical user follows an exponential distribution $h_{i,j} \sim \exp(1)$.

A. User Association

BSs in the i-th tier use the range expansion bias $B_i (i \in \mathcal{K})$ for CRE. The typical user is associated with the nearest BS of the k-th tier, where $k = \arg\max_{i \in \mathcal{K}} B_i P_i r_{i,0}^{-\alpha_i}$, $r_{i,0}$ is the distance between the typical user and the nearest BS in the i-th tier. This k-th tier typical user is classified as a Center Region User (CRU) if $P_k r_{k,0}^{-\alpha_k} > M_k^i P_i r_{i,0}^{-\alpha_i}$, $i \in \mathcal{K}/\{k\}$, and otherwise an Edge Region User (ERU). M_k^i is defined as the center region factor, which decides the center region area of a k-th tier cell. The value of M_k^i should be larger than B_i/B_k, so that the center region area of a k-th tier cell is smaller than the range-expanded coverage area of a k-th tier cell (influenced by B_i/B_k), and the resulting value of $A_k^{\mathrm{R}}/A_k^{\mathrm{F}}$ is comparable to that of $\beta_k/(1-\beta_k)$, where A_k^{R} and A_k^{F} respectively denote the probabilities of the typical user being a CRU and an ERU [4]. For small cells, the center region factor is set at $M_2^1 = 1$, so that the center area is the same as the original coverage area without CRE. CRUs and ERUs in each tier are respectively allocated with RPSs and FPSs, and the tier-1 RPSs and FPSs share the same transmitting slots with the tier-2 FPSs and RPSs, respectively. This is because that ERUs should be protected by BSs in the other tier transmitting RPSs. For example, the tier-2 ERUs suffer the FPS interference from other tier-2 BSs, and suffer the RPS interference from the tier-1 BSs. Consequently, the duty cycles follow $\beta_2 = 1 - \beta_1$.

B. Interference Caused By Subframe Misalignment

A full buffer traffic model is assumed for each BS, i.e., each BS always has data to transmit. Fig. 1 shows that due to SM, a serving subframe for a tier-1 typical user suffers interference from two consecutive subframes transmitted by a tier-1 BS. It can be extended to a more general case that a serving subframe for the k-th tier typical user suffers interference from two consecutive subframes transmitted by an i-th tier BS. We assume that the MSMO $T_{ki}^{\max}$ between an i-th tier interfering BS and a k-th tier user does not exceed the subframe duration T_p, i.e., $T_{ki}^{\max} \leq T_p$ [6]. For analytical tractability, the SM offset between an i-th tier BS and the k-th tier typical user is modelled as a uniformly distributed random variable in the range of $[0, T_{ki}^{\max}]$ [5]. We define $N_{ki} = T_p/T_{ki}^{\max}$ as the maximum SM factor. BSs in the same tier share the same value of N_{ki}. The signal-to-interference ratio (SIR) of the serving subframe for the k-th tier typical user is given by:

$$\Gamma_k^t = \frac{P_k^t h_{k,0} {r_{k,0}^t}^{-\alpha_k}}{\sum_{i \in K} \sum_{\mathbf{x}_{i,j} \in \Phi_i/\{\mathbf{x}_{k,0}\}} P_i \Delta_{i,j}^{k,t} h_{i,j} r_{i,j}^{-\alpha_i}}, \tag{1}$$

where $t \in \{\mathrm{R}, \mathrm{F}\}$. If $t = \mathrm{R}$, then the typical user is a CRU served by RPSs; otherwise it is an ERU served by FPSs. $P_k^{\mathrm{R}} = \rho_k P_k$, $P_k^{\mathrm{F}} = P_k$, and $\Delta_{i,j}^{k,t}$ is the random bias caused by SM on the received interference power from the j-th BS in tier i to the k-th tier CRU or ERU. In the following, we omit the BS index (i.e., the subscript j) from $\Delta_{i,j}^{k,t}$ and denote it by $\Delta_i^{k,t}$, because the SM offsets of BSs in the same tier are independent identically distributed.

For the two consecutive interfering subframes transmitted by an i-th tier BS, there are four different possible combinations: FPS and FPS, FPS and RPS, RPS and FPS, and RPS and RPS. Note that the type of one of the two consecutive interfering subframes can be determined because the SM offsets do not exceed the subframe duration. For example, if the typical user is a tier-1 CRU, then one of the two consecutive subframes must be an RPS from an interfering tier-1 BS, and must be an FPS from an interfering tier-2 BS. Herein we categorize the random bias $\Delta_i^{k,t}$ as the RPS random bias $\Delta_k^{\mathrm{R}}(i)$ or the FPS random bias $\Delta_k^{\mathrm{F}}(i)$ if the determined subframe in the two consecutive subframes is found to be an RPS or an FPS, respectively. According to the subframe allocation described in the user association strategy, we can determine the transformation between $\Delta_i^{k,t}$ and $\Delta_k^{t'}(i)$, $t' \in \{\mathrm{R}, \mathrm{F}\}$, as follows:

$$\Delta_i^{k,\mathrm{R}} = \begin{cases} \Delta_k^{\mathrm{R}}(i), i = k \\ \Delta_k^{\mathrm{F}}(i), i \neq k \end{cases}, \quad \Delta_i^{k,\mathrm{F}} = \begin{cases} \Delta_k^{\mathrm{F}}(i), i = k \\ \Delta_k^{\mathrm{R}}(i), i \neq k \end{cases}. \tag{2}$$

The randomness in $\Delta_k^{\mathrm{R}}(i)$ and $\Delta_k^{\mathrm{F}}(i)$ is caused by the undetermined subframe in the two consecutive interfering subframes. For the RPS random bias, if the undetermined subframe is an FPS, then $\Delta_k^{\mathrm{R}}(i)$ follows a uniform distribution in the range of $[\rho_i, \rho_i + \frac{1-\rho_i}{N_{ki}}]$, following the average interference power calculation in [8]; otherwise, $\Delta_k^{\mathrm{R}}(i) = 1$. For the FPS random bias, if the undetermined interfering subframe is an FPS, then $\Delta_k^{\mathrm{F}}(i) = 1$, and otherwise follows a uniform distribution in the range of $[1 - \frac{1-\rho_i}{N_{ki}}, 1]$. The Probability Density Functions (PDFs) of $\Delta_k^{\mathrm{F}}(i)$ and $\Delta_k^{\mathrm{R}}(i)$ are given as:

$$f_{\Delta_k^{\mathrm{F}}(i)}(\xi) = (1-\beta_i)\delta(\xi - 1) + \frac{\beta_i N_{ki}}{1-\rho_i} \mathbf{1}_{\xi \in [1 - \frac{1-\rho_i}{N_{ki}}, 1]}, \tag{3}$$

$$f_{\Delta_k^{\mathrm{R}}(i)}(\xi) = \beta_i \delta(\xi - \rho_i) + \frac{(1-\beta_i) N_{ki}}{1-\rho_i} \mathbf{1}_{\xi \in [\rho_i, \rho_i + \frac{1-\rho_i}{N_{ki}}]}, \tag{4}$$

where $\delta(\cdot)$ is the Dirac delta function, and $\mathbf{1}_z$ is the indicator function. The function $\mathbf{1}_z = 1$ if the subscript z is true, and otherwise $\mathbf{1}_z = 0$.

III. Coverage Probability Analysis

In this section, we analyse the coverage probability of the two-tier HetNet employing RPSs under SM. The coverage probability is defined as the probability that the SIR of the typical user is greater than a threshold τ, i.e., $\sum_{k\in\mathcal{K}}\sum_{t\in\{\mathrm{R,F}\}} A_k^t \mathbb{P}(\Gamma_k^t > \tau)$. The PDFs of the distance to the serving BS, conditioned on the typical tier-k user being a CRU or an ERU, i.e., $f_{r_{k,0}^{\mathrm{R}}}(r)$ and $f_{r_{k,0}^{\mathrm{F}}}(r)$, are respectively obtained as $f_{r_{k,0}^{\mathrm{R}}}(r) = \mathcal{D}(k, M_k^1, M_k^2, r)/A_k^{\mathrm{R}}$ and $f_{r_{k,0}^{\mathrm{F}}}(r) = (\mathcal{D}(k, \widehat{B}_1^k, \widehat{B}_2^k, r) - \mathcal{D}(k, M_k^1, M_k^2, r))/A_k^{\mathrm{F}}$, where $\widehat{B}_i^k = B_i/B_k$, $i \in \mathcal{K}$. These PDFs are obtained following similar steps in [9], with function $\mathcal{D}(\cdot)$ defined as:

$$\mathcal{D}(k, y_1, y_2, r) = 2\pi\lambda_k r \exp(-\pi \sum_{i\in\mathcal{K}} \lambda_i (y_i \widehat{P}_i^k)^{2/\alpha_i} r^{2/\widehat{\alpha}_i^k}), \quad (5)$$

where $\widehat{P}_i^k = P_i/P_k$, and $\widehat{\alpha}_i^k = \alpha_i/\alpha_k$. The probabilities A_k^{R} and A_k^{F} can be obtained in a way similar to Lemma 1 in [9] as $A_k^{\mathrm{R}} = \int_0^\infty \mathcal{D}(k, M_k^1, M_k^2, r)dr$ and $A_k^{\mathrm{F}} = \int_0^\infty \mathcal{D}(k, \widehat{B}_1^k, \widehat{B}_2^k, r)dr - A_k^{\mathrm{R}}$, respectively. Based on these conditional serving-BS-distance PDFs, the coverage probability of a tier-k CRU or ERU under SM is given in Theorem 1.

Theorem 1. *The coverage probability of the typical user in the k-th tier (as a CRU if $t = \mathrm{R}$ and as an ERU if $t = \mathrm{F}$) under SM is given as:*

$$\mathbb{P}(\Gamma_k^t > \tau) = \int_R \exp\left(-2\pi\lambda_i \sum_{i\in K} \mathcal{F}_{\Delta_i^{k,t}}(s_k^t(r))\right) f_{r_{k,0}^t}(r)dr, \quad (6)$$

where $s_k^t(r) = \tau r^{\alpha_k}/P_k^t$. For notational simplicity, s_k^t is used to replace $s_k^t(r)$ in the following. The function $\mathcal{F}_{\Delta_i^{k,t}}(s_k^t)$ can be transformed into $\mathcal{F}_{\Delta_k^R(i)}(s_k^t)$ or $\mathcal{F}_{\Delta_k^F(i)}(s_k^t)$ based on (2) as follows:

$$\mathcal{F}_{\Delta_k^R(i)}(s_k^t) = \beta_i \mathcal{G}_i(m_i^{k,t}, n_i^{k,t}) + (1-\beta_i)\mathcal{H}_i(\rho_i, \rho_i + \frac{1-\rho_i}{N_{ki}}, n_i^{k,t}), \quad (7)$$

$$\mathcal{F}_{\Delta_k^F(i)}(s_k^t) = (1-\beta_i)\mathcal{G}_i(m_i^{k,t}, n_i^{k,t}) + \beta_i \mathcal{H}_i(1 - \frac{1-\rho_i}{N_{ki}}, 1, n_i^{k,t}), \quad (8)$$

where $m_i^{k,t} = s_k^t P_i$, $n_i^{k,t} = (m_i^{k,t})^{-\frac{\alpha_i}{2}} (d_i^{k,t})^2$, $d_i^{k,t}$ is the minimum interfering distance, and is given by:

$$d_i^{k,t} = \begin{cases} (\widehat{P}_i^k M_k^i)^{\frac{1}{\alpha_i}} r_{k,0}^{\frac{1}{\widehat{\alpha}_i^k}}, i \neq k, t = R, \\ (\widehat{P}_i^k \widehat{B}_i^k)^{\frac{1}{\alpha_i}} r_{k,0}^{\frac{1}{\widehat{\alpha}_i^k}}, i \neq k, t = F, \\ r_{k,0}, \quad \textit{otherwise}. \end{cases} \quad (9)$$

The function $\mathcal{H}_i(b, c, y)$ is given in (12) at the top of next page, with the function $\mathcal{C}_i(b, c, y)$ represented as:

$$\mathcal{C}_i(b, c, y) = c\phi(-cy^{-\frac{\alpha_i}{2}}, 1, -\frac{2}{\alpha_i}) - b\phi(-by^{-\frac{\alpha_i}{2}}, 1, -\frac{2}{\alpha_i}), \quad (10)$$

where $\phi(\cdot)$ denotes the Lerch's Transcendent function [10]. Denoting ${}_2F^1(\cdot)$ as the Gauss hypergeometric function, the function $\mathcal{G}_i(a, y)$ in (7) and (8) is given as:

$$\mathcal{G}_i(a, y) = \frac{2a^{\frac{2}{\alpha_i}} y^{1-\frac{\alpha_i}{2}}}{\alpha_i - 2} {}_2F^1(1, 1 - \frac{2}{\alpha_i}; 2 - \frac{2}{\alpha_i}; -y^{-\frac{\alpha_i}{2}}). \quad (11)$$

Proof. See Appendix A. □

The coverage probability in (6) can be calculated numerically with a one-dimensional integration if pathloss exponents of the two tiers are different. Therefore, the coverage probability of a typical user, i.e., $\sum_{k\in\mathcal{K}}\sum_{t\in\{\mathrm{R,F}\}} A_k^t \mathbb{P}(\Gamma_k^t > \tau)$, can be analysed.

IV. Simulation Results

The simulated network area is a square of 400 km^2, with the tier-1 BS density λ_1 being 1 node/km^2. We simulate 10,000 realizations of the BS locations following the PPP, where the user is deployed at the origin, to obtain the complementary cumulative distribution function of the coverage probability. Note that in a full buffer traffic network, the MSMOs between a tier-2 BS and the typical user of each tier (i.e., N_{12} and N_{22}) have no effect on the coverage probability, thus they can be neglected in the discussion. We assume that the MSMOs between a tier-1 BS and the typical user of each tier, i.e., N_{11} and N_{21}, have the same value to simplify the discussion. Besides, a typical tier-1 CRU and tier-2 ERU are respectively referred to as a tier-1 victim user (VU) and a tier-2 VU, as they will suffer from increased interference due to SM.

Fig. 2 plots the analytical and simulated coverage probabilities of a typical user versus the SIR thresholds for the strict SA case ($N_{11} = \infty$) and the SM cases with $N_{11} = 1, 2$, under the low ($\lambda_2 = 10\lambda_1$) and the high ($\lambda_2 = 50\lambda_1$) small-cell density scenarios. It shows that the theoretical results closely match the simulation results, proving the effectiveness of our proposed SM model for analysing the coverage probability under SM. We can see that the SM causes severe coverage probability losses, especially in a low small-cell density scenario, in which the coverage probability declines approximately by 17% at 0 dB SIR threshold. In addition, the coverage losses caused by SM diminish with the increase of small-cell density.

Fig. 3 illustrates the theoretical coverage probabilities of VUs of both tiers versus N_{11} for $\rho_1 = 0.1$ and $\rho_1 = 0.3$ under $\lambda_2 = 10\lambda_1$ and $\lambda_2 = 50\lambda_1$. It shows that SM decreases coverage probabilities of VUs remarkably. The tier-2 VU in a low small-cell density scenario suffers a maximum 20% coverage probability reduction. Moreover, a larger power reduction factor ρ_1 alleviates the coverage probability degradation of VUs of both tiers caused by SM, but the coverage probability of a tier-2 VU becomes undesirably poor. In addition, the coverage probabilities of VUs decrease with the increase of the MSMO, regardless of the small-cell density. According to the coverage probabilities of VUs of both tiers with $\rho_1 = 0.1$ and $\lambda_2 = 10\lambda_1$, in which the effect of SM is the most significant as observed in Fig. 2, we can see that the strict SA requirement can be relaxed by up to 20% of a subframe duration, while ensuring the coverage losses caused by SM below 5%.

V. Conclusion

In this letter, we have analysed the downlink coverage probability for a two-tier HetNet employing RPSs under SM. Our analytical and simulation results show that the SM will significantly decrease the coverage probability of a typical user, which can be mitigated by increasing the small-cell density. However, the coverage losses of VUs of both tiers caused by SM cannot be mitigated by increasing the small-cell density, but it can be reduced by increasing the tier-1 power reduction factor. Unfortunately, the coverage probability of a small-cell CRE user will be degraded if the tier-1 power reduction factor increases. For protecting the VUs with below 5% coverage reduction caused by SM, the SA requirement can be relaxed by up to 20% of the subframe duration.

$$\mathcal{H}_i(b,c,y) = \frac{\alpha_i y^{\frac{\alpha_i+2}{2}}}{(\alpha_i+2)(b-c)}\left(\frac{1}{2}(\alpha_i+2)(c-b)y^{-\frac{\alpha_i}{2}} + \log(by^{-\frac{\alpha_i}{2}}+1) - \log(cy^{-\frac{\alpha_i}{2}}+1) + y^{-\frac{\alpha_i}{2}}\mathcal{C}_i(b,c,y)\right) \tag{12}$$

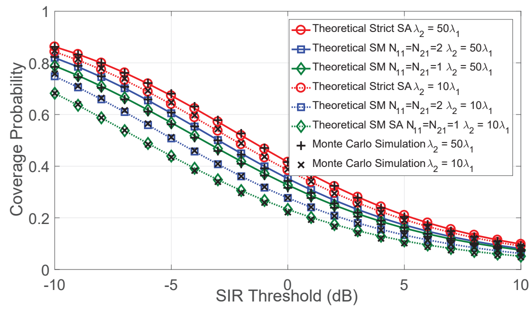

Fig. 2. Coverage probability validation of a typical user under SM, where $\lambda_1 = 1$ node/km^2, $P_1 = 100P_2$, $B_2 = 4B_1$, $[M_1^2, M_2^1] = [20,1]$, $[\rho_1,\rho_2] = [0.1,1]$, $[\beta_1,\beta_2] = [0.5,0.5]$, and $[\alpha_1,\alpha_2] = [3,4]$.

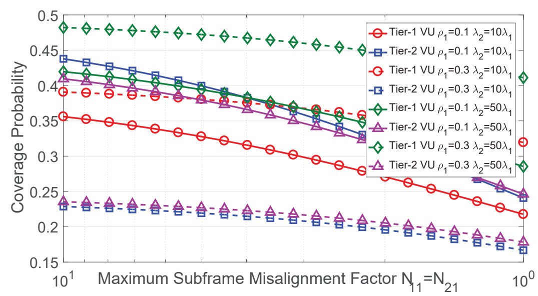

Fig. 3. The theoretical coverage probabilities of VUs versus the maximum SM factor N_{11}, with $\lambda_1 = 1$ node/km^2, $P_1 = 100P_2$, $B_2 = 4B_1$, $[M_1^2, M_2^1] = [20,1]$, $\tau = 0$ dB, $\rho_2 = 1$, $[\beta_1,\beta_2] = [0.5,0.5]$, and $[\alpha_1,\alpha_2] = [3,4]$.

Appendix A
Proof of Theorem 1

According to the definition in Section III, the coverage probability of the k-th tier user can be calculated as follows:

$$\mathbb{P}(\Gamma_k^t > \tau) = \int_R \prod_{i\in K} \mathbb{E}[e^{-s_k^t I_{i,k}^t}] f_{r_{k,0}}^t(r)dr, \tag{13}$$

where $I_{i,k}^t$ denotes the aggregate interference power of the i-th tier BSs on the k-th tier CRU or ERU. Then the result is transformed into a form with the product of Laplace Transforms (LTs) of the aggregate interference power of each tier. The LT $\mathcal{L}_{I_{i,k}^t}(s_k^t), i \in \mathcal{K}$, can be represented as follows:

$$\mathcal{L}_{I_{i,k}^t}(s_k^t) = \exp(-2\pi\lambda_i \int_{d_i^{k,t}}^{\infty} (1 - \mathbb{E}_{h,\Delta}[e^{-s_k^t P_i h_i \Delta_i^{k,t} u^{-\alpha_i}}])udu), \tag{14}$$

which is obtained by the moment generating function [7]. By substituting $\int_{d_i^{k,t}}^{\infty}(1-\mathbb{E}_{h,\Delta}[e^{-s_k^t P_i h_i \Delta_i^{k,t} u^{-\alpha_i}}])udu$ with $\mathcal{F}_{\Delta_i^{k,t}}(s_k^t)$, we have $\mathcal{L}_{I_i}(s_k^t) = \exp(-2\pi\lambda_i \mathcal{F}_{\Delta_i^{k,t}}(s_k^t))$. Equipped with the transformation between $\Delta_i^{k,t}$ and $\Delta_k^{t'}(i)$ as in (2), the expectation $\mathbb{E}_{h,\Delta}[\exp(-\omega_i^{k,t} h_i \Delta_i^{k,t})]$ in (14) can be calculated as follows with $\omega_i^{k,t} = s_k^t P_i u^{-\alpha_i}$:

$$\mathbb{E}_\Delta[\mathbb{E}_{h_i}[\exp(-\omega_i^{k,t}\Delta_k^{t'}(i)h_i)]] = \mathbb{E}_\Delta\left[(1+\omega_i^{k,t}\Delta_k^{t'}(i))^{-1}\right]. \tag{15}$$

Based on (3) and (4), the expression in (15) can be respectively transformed into $(1-\beta_i)\frac{1}{1+\omega_i^{k,t}} + \beta_i \int_{1-\frac{1-\rho_i}{N_k i}}^{1} \frac{1}{1+\omega_i^{k,t}\xi}\frac{N_{ki}}{1-\rho_i}d\xi$ and $\beta_i \frac{1}{1+\rho_i\omega_i^{k,t}} + (1-\beta_i)\int_{\rho_i}^{\rho_i+\frac{1-\rho_i}{N_{ki}}} \frac{1}{1+\omega_i^t\xi}\frac{N_{ki}}{1-\rho_i}d\xi$ with $t' =$ F and R. Then by calculating the integrals in these two results, the defined function $\mathcal{F}_{\Delta_i^{k,t}}(s_k^t)$, combined with (15), can be generally denoted by $\mathcal{F}_{\Delta_k^{t'}(i)}(a,b,c)$ as:

$$\mathcal{F}_{\Delta_k^{t'}(i)}(a,b,c) = \int_{d_i^{k,t}}^{\infty} (\tilde{\beta}_i^{t'}\mathcal{Q}_i^1(a) + (1-\tilde{\beta}_i^{t'})\mathcal{Q}_i^2(b,c))udu, \tag{16}$$

where $\{\tilde{\beta}_i^{\mathrm{R}}, \tilde{\beta}_i^{\mathrm{F}}\} = \{\beta_i, 1-\beta_i\}$, a, b and c are three parameters with $a \in \{\rho_i, 1\}$, $b \in \{\rho_i, 1-\frac{1-\rho_i}{N_k i}\}$, and $c \in \{\rho_i + \frac{1-\rho_i}{N_{ki}}, 1\}$, $\mathcal{Q}_i^1(a) = 1 - 1/(1+a\omega_i^{k,t})$, and $\mathcal{Q}_i^2(b,c)$ is given by:

$$\mathcal{Q}_i^2(b,c) = 1 - \frac{\ln(1+c\omega_i^{k,t}) - \ln(1+b\omega_i^{k,t})}{(c-b)\omega_i^{k,t}}. \tag{17}$$

The closed form result of function $\int_{d_i^{k,t}}^{\infty} \mathcal{Q}_i^1(a)udu$ can be easily obtained as $G_i(a, n_i^{k,t})$ [4]. Moreover, we have:

$$\int_{d_i^{k,t}}^{\infty} \mathcal{Q}_i^2(b,c)udu =$$
$$\frac{m_i^{k,t\,\frac{2}{\alpha_i}}}{\alpha_i}\int_0^{n_i^{k,t\,-\frac{2}{\alpha_i}}} \left[1 - \frac{\ln(1+c\omega) - \ln(1+b\omega)}{(c-b)\omega}\right]\omega^{-\frac{2+\alpha_i}{\alpha_i}}d\omega, \tag{18}$$

which can be transformed into $\mathcal{H}_i(b,c,n_i^{k,t})$ as expressed in (12) by symbolic integration in Wolfram Mathematica. Equipped with $G_i(a, n_i^{k,t})$ and $\mathcal{H}_i(b,c,n_i^{k,t})$, the result of function $\mathcal{F}_{\Delta_k^{t'}(i)}(a,b,c)$ in (16) can be achieved. As a result, we can obtain the LTs of the aggregate interference power $L_{I_i}(s_k^t)$, $i \in \mathcal{K}$, as in (14). Then by incorporating the result of $L_{I_i}(s_k^t)$ into (13), the result in Theorem 1 can be yielded.

References

[1] D. Lopez-Perez et al., "Enhanced intercell interference coordination challenges in heterogeneous networks," *IEEE Wireless Commun.*, vol. 18, pp. 22–30, June 2011.

[2] A. Merwaday, S. Mukherjee, and I. Guvenc, "Hetnet capacity with reduced power subframes," in *IEEE WCNC 2014*, pp. 1380–1385.

[3] D. Bladsjö, M. Hogan, and S. Ruffini, "Synchronization aspects in LTE small cells," *IEEE Commun. Mag.*, vol. 51, pp. 70–77, Sep. 2013.

[4] H. Hu, J. Weng, and J. Zhang, "Coverage performance analysis of feicic low-power subframes," *IEEE Trans. Wireless Commun.*, vol. 15, pp. 5603–5614, Aug 2016.

[5] V. Naghshin et al., "Downlink coverage analysis of two-tier heterogeneous networks with asynchronous slots," in *IEEE ICC 2016*, pp. 1–6.

[6] X. Lin, L. Jiang, and J. G. Andrews, "Performance analysis of asynchronous multicarrier wireless networks," *IEEE Trans. Commun.*, vol. 63, pp. 3377–3390, Sept 2015.

[7] J. G. Andrews, F. Baccelli, and R. K. Ganti, "A tractable approach to coverage and rate in cellular networks," *IEEE Trans. Commun.*, vol. 59, pp. 3122–3134, Nov. 2011.

[8] B. Błaszczyszyn and P. Mühlethaler, "Interference and SINR coverage in spatial non-slotted Aloha networks," *annals of telecommun.-annales des télécommun.*, vol. 70, pp. 345–358, Aug. 2015.

[9] S. Singh and J. G. Andrews, "Joint resource partitioning and offloading in heterogeneous cellular networks," *IEEE Trans. Wireless Commu.*, vol. 13, pp. 888–901, February 2014.

[10] E. Ferreira, A. Kohara, and J. Sesma, "New properties of the Lerch's transcendent," *J. of Number Theory*, vol. 172, pp. 21–31, Mar. 2017.